Proc. of the 8th International Symposium on Geotechnical Safety and Risk (ISGSR)
Edited by Jinsong Huang, D.V. Griffiths, Shui-Hua Jiang, Anna Giacomini and Richard Kelly
 Published by Research Publishing, Singapore.
doi: 10.3850/978-981-18-5182-7_22-002-cd

ISGSR 2022

Stability Analysis and Failure Mechanism of Three-Dimensional Heterogeneous Slope Under Steady State Rainfall

Cheng Qian[1] and Yajun Li[1]

[1]School of Engineering and Technology, China University of Geosciences, Beijing, Beijing, China.
E-mail: qiancheng@cugb.edu.cn
E-mail: y.j.li@cugb.edu.cn

Abstract: Matrix suction contributes to the stability of unsaturated soil slopes. It is generally accepted that rainfall infiltration will reduce the matrix suction of the soil and lead to the instability and failure of the unsaturated soil slope. The van Genuchten model can be used to characterize the relationship of matrix suction with saturation. Previous studies mainly focused on two-dimensional unsaturated soil slopes, which can not consider the impact of the variability of parameters in three-dimensional space on slope stability. The 2D simplification makes the research relatively simple and deviates from the real situation. In the actual slope, the parameters such as saturated hydraulic conductivity, and of van Genuchten model have 3D spatial variability, and affects rainfall infiltration. The heterogeneity of these parameters leads to the heterogeneity distribution of matrix suction in space, so the spatial distribution of soil strength is also heterogeneous. Previous sensitivity analysis studies show that in the three parameters of saturated hydraulic conductivity, and of van Genuchten model, has a greater influence on the distribution of matrix suction than the other two. The research in this paper is focused on an ideal 3D unsaturated slope under steady state rainfall, and compared with 2D model. Monte-Carlo method and random fields are used to randomly simulate the spatial distribution field of , steady state flow is calculated in COMSOL, and the suction stress is brought into the finite element program to calculate the slope stability. The results show that the spatial variability of the affects the deformation and failure surface location of the 3D unsaturated soil slope. The analysis of 3D slope deformation mechanism shows that the deformation and failure of unsaturated soil slope occur in the region with weak suction.

Keywords: Three-dimensional slope; Unsaturated slope; Hydraulic parameters; deformation mechanism.

1 Introduction

The stability analysis of unsaturated slope under rainfall infiltration is an important part of geotechnical engineering, but the assumed ideal model is different from the actual slope. One of the sources of uncertainty in the analysis is the spatial variability of hydraulic parameters. Therefore, this article has major research on the influence of 3D spatial variability of hydraulic parameters on unsaturated slope failure.

The deposition of soil is not uniform under natural conditions, which leads to the soil parameters are uneven in 3D space. Due to the limitation of engineering conditions, the soil parameters measured in the field or laboratory are limited, which is difficult to reflect the spatial variability of parameters. Therefore, in the traditional stability analysis methods, the parameters are usually regarded as deterministic to simplify the analysis, which would lead to some results deviate from the actual situation. In recent years, with the development of random field theory, it is more and more common to study the stability of slope considering the spatial variability of parameters.

The heterogeneity of soil parameters makes it inevitable that there are weakness region in the soil. Therefore, the failure often occurs in the weak parts of the soil. In unsaturated heterogeneous slopes, rainfall infiltrates preferentially along the path of high permeability areas rather than uniform infiltration, resulting in spatially irregular matrix suction in the soil (Le et al. 2012).

The uncertainty of soil material will affect the failure form of unsaturated slope. Many of them used the finite element method (FEM) to analyze the impact of strength changes on slope safety (Hicks 2005; Griffiths and Fenton 2004). The complex variation model of soil parameters was generated by Monte-Carlo simulation, and the uncertainty of heterogeneous slope was studied. These simulation results showed that the heterogeneity of materials had a great impact on the stability of soil slopes (Griffiths and Fenton 2004; Fenton and Griffiths 2005; Griffiths et al. 2015). Much work based on Monte-Carlo simulation focuses on these processes and the failure or reliability of fully saturated heterogeneous slopes (Griffiths and Fenton 2004; Hicks and Onisphorou 2005; Hicks and Samy 2002). Hicks et al. (2008) proposed a 3D random study on the sliding region of saturated slope. In unsaturated slope, soil permeability, rainfall intensity and rainfall time have a significant impact on the stability of unsaturated slope. Patrick and Hicks (2010) analyzed the effects of different factors (groundwater level position and soil air entry value) on slope failure. Le et al. (2015) evaluated the effect of spatial variability of porosity on the stability and failure consequences of unsaturated slopes, based on this research, Le et al. (2019) studied the effects of other parameters on the stability and failure consequences of unsaturated slope, and considered the location of wetting front and slope failure mechanism.

2 Method

The main purpose of this paper is to explore the influence of spatial variability of soil parameters on unsaturated slope failure. Therefore, using a simple mechanical model and hydraulic model in this paper.

2.1 Shear strength

Mohr-Coulomb model is adopted for the material of soil, and Bishop effective stress equation is adopted for the mechanical constitutive relationship. The failure criterion extended for unsaturated conditions is :

$$\tau_f = c' + (\sigma - u_a)\tan\phi' + \chi(u_a - u_w)\tan\phi' \tag{1}$$

where σ_f is the soil shear strength, c' is the effective cohesion, ϕ' is the effective angle of friction, σ is the total stress, u_a is the pore air pressure, u_w is the pore water pressure, $(\sigma - u_a)$ is the net stress and $(u_a - u_w)$ is the matric suction. The effective stress parameter χ can be expressed as $\chi = \Theta_N^{\kappa}$ (Vanapalli et al. 1996; Fredlund et al. 1996), where Θ_N is the effective saturation, and κ is a fitting parameter.

2.2 Retention Models

The Soil-Water Characteristic Curve (SWCC) has been modeled using the relationship proposed by van Genuchten (1980), the expression in COMSOL is:

$$\theta = \begin{cases} \theta_r + S_e(\theta_s - \theta_r) & H_p < 0 \\ \theta_s & H_p \geq 0 \end{cases} \tag{2}$$

$$S_e = \begin{cases} \dfrac{1}{\left[1 + \left|\alpha H_p\right|^n\right]^m} & H_p < 0 \\ 1 & H_p \geq 0 \end{cases} \tag{3}$$

where θ is the actual volumetric water content, θ_s and θ_r represent the volumetric water contents at the saturated and residual conditions respectively, S_e is effective saturation. α , n and $m = 1 - 1/n$ are fitting parameters. C_m is specific moisture capacity.

$$C_m \begin{cases} \dfrac{\alpha m}{1-m}(\theta_s - \theta_r) S_e^{\frac{1}{m}} \left(1 - S_e^{\frac{1}{m}}\right)^m & H_p < 0 \\ 1 & H_p \geq 0 \end{cases} \tag{4}$$

The hydraulic conductivity $k(s)$ at a given suction level is :

$$k(s) = k(r) k_{sat} \tag{5}$$

$$k_r = \begin{cases} S_e^l \left[1 - \left(1 - S_e^{\frac{1}{m}}\right)^m\right]^2 & H_p < 0 \\ 1 & H_p \geq 0 \end{cases} \tag{6}$$

Where k_{sat} is the saturated hydraulic conductivity.

2.3 Richards' equation

In this paper, the rainfall rate of vertical infiltration is q , subsurface water flow in the unsaturated zone and in groundwater is governed by the Richards' equation :

$$\rho\left(\frac{C_m}{\rho g} + S_e S\right)\frac{\partial p}{\partial t} + \nabla \cdot \rho\left(-\frac{K_s}{\mu} k_r (\nabla p + \rho g \nabla D)\right) = Q_m \tag{7}$$

In this equation, pressure p is the dependent variable, C_m represents the specific moisture capacity, S_e is effective saturation, S is the storage coefficient, water storage is not considered in this paper, so $S=0$. μ is the fluid dynamic viscosity, k_r denotes the relative permeability, ρ is the fluid density, g is acceleration of gravity, D represents the elevation, and Q_m is the fluid source.

2.4 Summary of material parameters

Table 1 lists the typical average values of sandy silt and includes the relevant parameters of SWCC.

Table 1. Model parameters

Parameter	Describe	Value	Unit	Parameter	Describe	Value	Unit
γ	Soil unit weight	20	$[kN/m^3]$	c'	Effective cohesion	10	$[kPa]$
E	Young's modulus	5×10^4	$[kPa]$	κ	Fitting parameter	1.0	$[-]$
ν	Poisson's ratio	0.3	$[-]$	k_{sat}	Sat. Hydr. conductivity	8×10^{-6}	$[m/s]$
ψ	Dilation angle	0	[°]	α	Fitting parameter	0.5	$[m^{-1}]$
ϕ'	Effective friction angle	25	[°]	n	Fitting parameter	4.0	$[-]$

3 Randomization parameters

The spatial variability of SWCC parameters is generally expressed by assumed probability distribution, point statistics and spatial statistics. The point statistics are the mean μ and standard deviation σ of the parameters, which can be combined to obtain the coefficient of variation:

$$V=\frac{\sigma}{\mu} \tag{8}$$

Spatial statistics is the scale of fluctuation (SOF) in the coordinate direction. The SOF indicates the correlation degree of soil within a certain range. The larger the SOF of soil parameters, the larger the range of strong parameter correlation, which indicating that the soil is more uniform. In this paper, random fields are generated based on the Local Average Subdivision method (LAS) (Fenton and Vanmarcke 1998). Hicks and Samy (2002, 2004) describe the generation of anisotropic random fields.

Zhu and Mohanty (2003) found that the impact of the variability in α is lager than that of n. Zhang (2002) found that among the parameters affecting slope stability, unsaturated parameter α is more sensitive than saturated hydraulic conductivity k_{sat}. To sum up, taking 2D and 3D slopes as the main research object, considering the spatial variability of parameters α, this paper compared the differences of 2D and 3D slope. Table 2 lists the distributions and point statistics selected for the analysis.

Table 2. Assumed distributions and point statistics

Parameter α	V	SOF (m)	Anisotropy		Distribution
			X	Y	
2D Model	0.5	1.0	12	12	Log-normal
3D Model	0.5	1.0	12	—	Log-normal

4 Numerical simulation

The research steps of this paper are as follows :

(1) The random field of SWCC parameters α is generated by LAS, the number of realization of 2D model and 3D model is both $N=100$;

(2) The random field is imported into COMSOL, and calculated steady-state rainfall infiltration;

(3) The suction is brought into the finite element program, and the strength reduction method is used to calculate the slope stability.

The model and boundary conditions in this paper are shown in Figure 1. The height of the slope is 5m, the groundwater level is located at 4m, rainfall infiltrates from the slope surface, the infiltration rate is $q=5.6\times10^{-7}m/s$. The 2D slope mesh adopts 8-node quadrilateral element. The 3D slope mesh adopts

20-node hexahedron element, roller boundary around the slope and fixed boundary at the bottom.

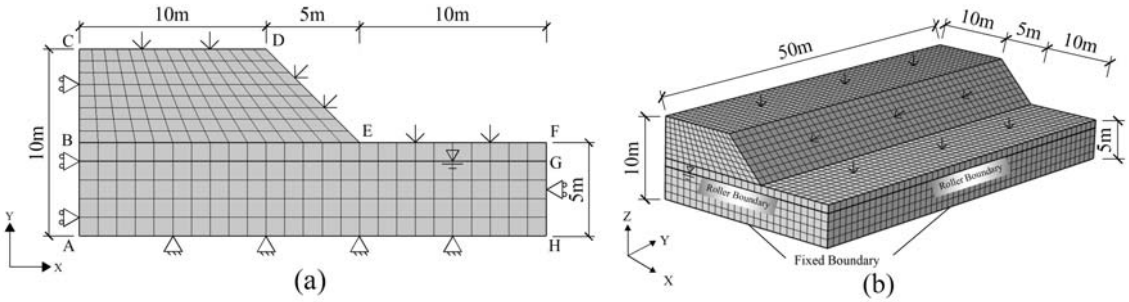

Figure 1. Model size, boundary conditions and finite element discretization ((a)2D model (b)3D model)

The slope material properties are defined in Table 1 and Table 2. The size of the random field element is similar to the finite element mesh. The interpolation function in COMSOL is used to assign the value of the centroid of the random field element to model. Figure 2 shows the typical random field of α , Red indicates the area with large value.

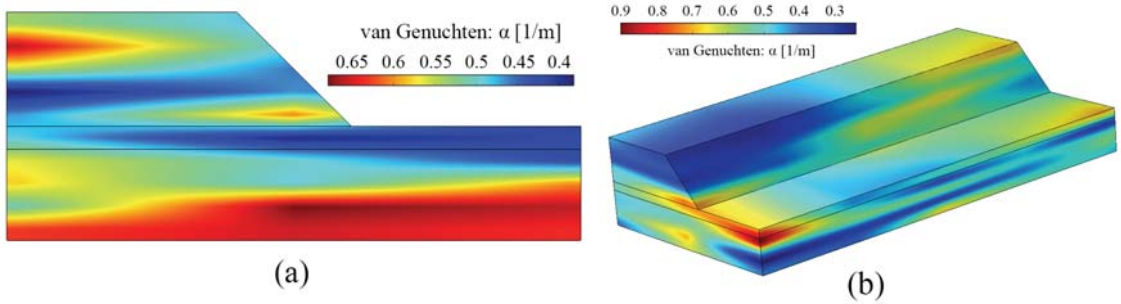

Figure 2. A typical random field of α ((a)2D model (b)3D model)

Brought the random field that shown in Figure 2 into the Richards' equation and calculated, the results of suction stress is shown in Figure 3. The suction stress below the groundwater level is zero, and red indicates the large value. Comparing suction stress of the 2D model and 3D model, it can be seen that the 3D random field of parameters is not a simple 2D expansion. Due to the random characteristics of parameters, the distribution of suction stress in space is not uniform, and the contribution to shear strength varies in space.

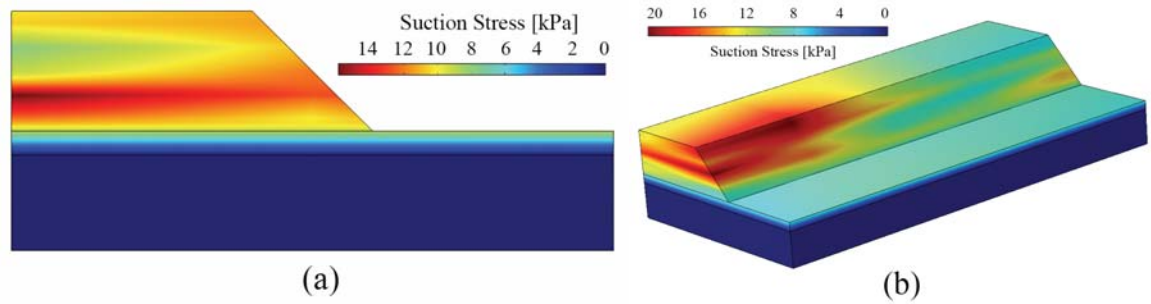

Figure 3. Fields of suction stress ((a)2D model (b)3D model)

The factor of safety (FOS) of the slope is calculated and the probability density function (PDF) of FOS for 2D and 3D slopes is shown in Figure 4, where E_{2D} and E_{3D} respectively represents the statistical mean of FOS of the 2D and 3D slope, σ_{2D} and σ_{3D} respectively represents the statistical standard deviation of FOS of the 2D and 3D slope, and N is the number of realization. The SOF of 2D slope equivalent to parameters is infinite in the third dimension, and the standard deviation of its FOS is greater than that of 3D slope.

As can be seen from Figure 5, the displacement at the toe of the slope is the largest. When considering the 3D spatial variability of parameters, the deformation and failure of slopes often occur in local weak region. It can be found from Eq.1 that that is because the suction stress in the unsaturated zone contributes to the shear strength of the slope. The region with small suction has low shear strength and is easily to deformation and failure.

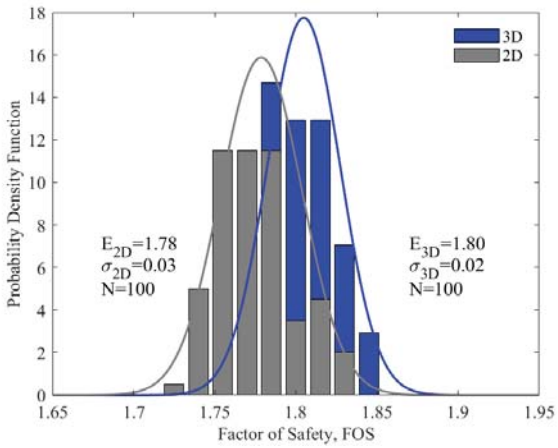

Figure 4. Probability density function of 2D and 3D slope

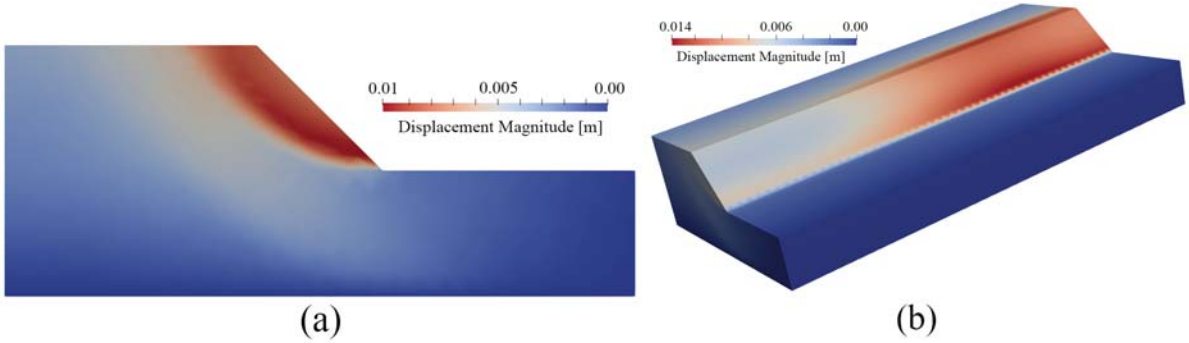

Figure 5. Displacement field ((a)2D model (b)3D model)

Figure 6 shows the equivalent plastic strain of the 3D slope. The deformation first occurs in the region with low suction, and the large value region in the equivalent plastic strain diagram reflects the large historical cumulative deformation in this region in the process of stability analysis.

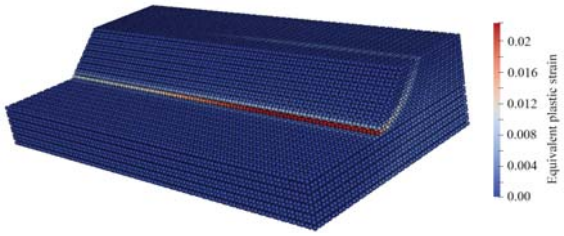

Figure 6. Equivalent plastic strain of 3D model

Along the Y-coordinate direction (Y=50.0m), it is divided into 50 sections with the complete unit as the boundary. After the 3D slope stability calculation, the maximum displacement of nodes on each section is output. The random fields of each section are brought into the 2D stability program to calculate the FOS. The statistical results are shown in Figure 7, where the right ordinate Max_disp represents the maximum displacement of the node on the section. According to the section statistical calculation results, the section with the lowest FOS is the most unfavorable section in the 3D slope, and the node displacement of this section is also the largest.

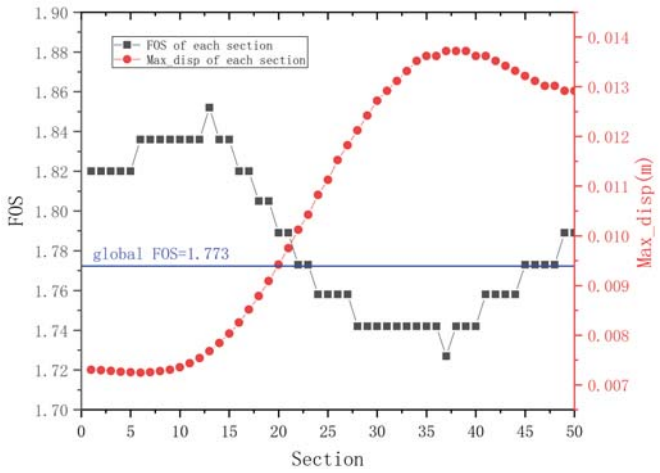

Figure 7. Maximum displacement and FOS of each section

5 Conclusions

This paper studies the influence of spatial variability of SWCC parameters α on 2D and 3D slope deformation under rainfall infiltration. The conclusions are as follows: (1)The spatial variability of parameters leads to different deformation (failure) results of 2D and 3D slopes, the 3D situation is not the simple extension of 2D; (2)The deformation (failure) develops along the weak suction stress part of the soil; (3)The spatial variability of parameters will change the deformation (failure) surface and scale of deformation (failure) volume.

References

Arnold, P. and Hicks, M.A. (2010). Stochastic modelling of unsaturated slope stability. *Paper presented at the Fifth International Conference on Unsaturated Soils, Barcelona, Spain*.

Fenton, G.A. and Griffiths, D.V. (2005). A slope stability reliability model. *In: Proceeding of the K.Y.Lo Symposium, London, Ontario*.

Fenton, G.A. and Vanmarcke, E.H. (1998). Spatial variation in liquefaction risk. *Geotechnique,* 46(6), 819-831.

Fredlund, D.G., Xing, A., Fredlund, M.D., et al. (1996). The relationship of the unsaturated soil shear strength to the soil-water characteristic curve. *Canadian Geotechnical Journal,* 33(3), 440-448.

Griffiths, D.V. and Fenton, G.A. (2004). Probabilistic slope stability analysis by finite elements. *Journal of Geotechnical and Geoenvironmental Engineering,* 130(5), 507-518.

Griffiths, D.V., Jinsong, H. and Fenton, G.A. (2015). Probabilistic slope stability analysis using RFEM with non-stationary random fields. *Geotechnical Safety and Risk V,* 704-709.

Hicks, M.A. (2005). Risk and variability in geotechnical engineering. *Geotechnique,* 1(55), 1-2.

Hicks, M.A., Chen, J. and Spencer, W.A. (2008). Influence of spatial variability on 3D slope failures. *Sixth International Conference on Computer Simulation Risk Analysis and Hazard Mitigation,* 335-342.

Hicks, M.A. and Onisiphorou, C. (2005). Stochastic evaluation of static liquefaction in a predominantly dilative sand fill. *Geotechnique,* 55(2), 123-133.

Hicks, M.A. and Samy, K. (2002). Influence of heterogeneity on undrained clay slope stability. *Quarterly Journal of Engineering Geology and Hydrogeology,* 35(1), 41-49.

Hicks, M.A. and Samy, K. (2004). Stochastic evaluation of heterogeneous slope stability. *Italian Geotechnical Journal*, 38(2), 54-66.

Le, T.M.H., Gallipoli, D., Sanchez, M., et al. (2012). Stochastic analysis of unsaturated seepage through randomly heterogeneous earth embankments. *International Journal for Numerical and Analytical Methods in Geomechanics*, 36(8), 1056-1076.

Le, T.M.H., Gallipoli, D., Sanchez, M., et al. (2015). Stability and failure mass of unsaturated heterogeneous slopes. *Canadian Geotechnical Journal*, 1-15.

Le, T.M.H., Sanchez, M., Gallipoli, D., et al. (2019). Probabilistic Study of Rainfall-Triggered Instabilities in Randomly Heterogeneous Unsaturated Finite Slopes. *Transport in Porous Media*, 126(1), 199-222.

Vanapalli, S.K., Fredlund, D.G., Pufahl, D.E., et al. (1996). Model for the prediction of shear strength with respect to soil suction. *Canadian Geotechnical Journal*, 33(3), 379-392.

van Genuchten, M.T. (1980). A closed-form equation for predicting the hydraulic conductivity of unsaturated soils. *Soil Science Society of America Journal 44,* 892-898.

Zhang, D. (2002). *Stochastic Methods for Flow in Porous Media. San Diego: Academic Press*, 297-325.

Zhu, J. and Mohanty, B.P. (2003). Effective hydraulic parameters for steady state vertical flow in heterogeneous soils. *Water Resources Research*, 39(8), 715-729.